Pattern Recognition 60 (2016) 648–656

Contents lists available at ScienceDirect

Pattern Recognition

journal homepage: www.elsevier.com/locate/pr

Mass classification in mammograms based on two-concentric masks and discriminating texton

Yanfeng Li [a], Houjin Chen [a,*], Xueye Wei [a], Yahui Peng [a], Lin Cheng [b]

[a] School of Electronic and Information Engineering, Beijing Jiaotong University, Beijing, China
[b] Center for Breast, People's Hospital of Peking University, Beijing, China

ARTICLE INFO

Article history:
Received 7 July 2015
Received in revised form
24 June 2016
Accepted 24 June 2016
Available online 25 June 2016

Keywords:
Concentric mask
Discriminating
Mammogram
Mass classification
Texton

ABSTRACT

In this paper, a mass classification method in mammograms is proposed based on two-concentric masks and discriminating texton. First, the two-concentric masks are employed, dividing each mass region into the center region and the periphery region. Then integrating linear discriminant analysis (LDA) with traditional texton, the discriminating texton is proposed. The shortage of not considering the class information in traditional texton is improved. Finally, features are extracted with discriminating texton for both the center region and the periphery region. Thus, the problem of disregarding the spatial layout information is alleviated. The proposed method is tested on 130 mass regions from Digital Database for Screening Mammography (DDSM) database. The classification accuracy rate reaches 86.92% and the area under the receiver operating characteristics (ROC) curve is 0.91, which is higher than traditional texton and some other texture-based methods.

1. Introduction

Breast cancer is one of the most common tumors among women. And it is the leading cause of cancerous deaths among women between 20 and 59 [1]. In recent years, the morbidity of breast cancer has an increasing trend, whereas the mortality has declined. This can be associated with the early detection and diagnosis. Among many imaging techniques, mammography is the one of the standard approaches for preliminary examination of breast cancer in women without symptoms [2].

The main signature of a breast tumor is usually indicated by the presence of a dense mass or a change in the texture in the mammogram [3]. Normally, a breast tumor is identified as benign or malignant through biopsy. Due to the traumatic nature and the cost of the biopsy, it would be valuable to develop a computer aided method to classify the tumors as benign or malignant [4]. When combining the radiologist's experience with the classification result given by a computer, a more comprehensive diagnosis can be obtained. However, accurate breast cancer classification is still challenging due to the unknown cause of the disease and the similarities between benign and malignant masses [1]. In this paper, classifying a mass region in the mammogram as benign or malignant was studied.

Several methods have been proposed for this topic. Based on the extracted feature, works can be divided into two types: shape-based methods and texture-based methods. For the shape-based methods, the basic idea is that a benign mass is normally round or oval and has a well-defined boundary, whereas a typical malignant tumor is spiculate and has a blurry boundary. Related to the shape difference between the benign masses and the malignant masses, Fourier descriptor, spiculate index and other shape features [5–7] have been designed and employed to classify masses in the mammograms. To obtain the shape features, mass contours have to be segmented first. And the segmentation should be accurate enough to guarantee high classification performance. Segmenting the mass contour is hard to be done automatically and accurately in clinical practice, as masses are often overlapped by the glandular tissues. For these reasons, texture-based methods may be good alternatives.

In texture-based classification, Mohanty et al. [8] extracted several first-order statistic features from the histogram and twenty texture features from the gray level co-occurrence matrix (GLCM) of the mass region. The first-order statistic features were mean, variance, skewness, kurtosis, entropy, and energy. In another paper of Mohanty et al. [9], features based on GLCM and gray level run length matrix (GLRLM) were studied. In the paper of Jaleel [10], six features computed from GLCM were extracted and used to tell benign and malignant masses apart. All the features mentioned above are the statistical characteristic of the gray value of the pixels. The classification performance for this type of features is not satisfactory. Mass classification based on statistical features is done in the space domain. Feature extracted from another

* Corresponding author.
E-mail address: hjchen@bjtu.edu.cn (H. Chen).

http://dx.doi.org/10.1016/j.patcog.2016.06.021
0031-3203/

domain naturally becomes a good alternative for the same task. Shanthi et al. [11] computed the multi-scale surrounding region dependence (SRD) matrices from the sub-bands of the wavelet transform. Then features were extracted from the computed matrices to classify masses as benign or malignant. Nascimento et al. [12] combined wavelet transform with singular value decomposition to extract features. In [13,14], images were first transformed to the curvelet domain and then the transformed coefficients were used as the features inputting into the classifier. Another type of feature extraction methods is based on filter response. In [15,16], features computed from the response to a bank of Gabor filters were used to classify masses. Besides statistical features, features extracted from the transformed domains and calculated by using filter-based methods, small texture descriptors showed promising performance in mass classification. These texture descriptors included local binary pattern (LBP), local ternary pattern (LTP), local phase quantization (LPQ) [17] and texton [18]. Small texture descriptors model one image as a histogram. An obvious disadvantage for this type of features is the disregard of the spatial layout information. Recently, deep learning method [19] has been applied to differentiate benign tumor from malignant tumor and obtains good result. Besides, some novel texture features [20,21] can also be employed for mass classification.

For a clinical application, a system is desirable, which can complete the classification without precisely segmenting the mass contour. To meet the need of the clinical applications and alleviate the problems in the existing methods, a mass classification method is proposed in this paper. This method combines two-concentric masks with discriminating texton. Texton achieves good performance in many texture analysis problems. However its dictionary construction step and texton quantization step do not consider the class information in the training samples. Linear discriminant analysis (LDA) is a supervised linear analysis method and can learn the discriminating information among the training samples. Adding the information learned by LDA to traditional texton, the discriminating texton is proposed. Another problem of texton is the disregard of the spatial layout information. Based on the growth characteristic of the mass, two-concentric masks are designed. These masks divide the whole mass region into the center region and the periphery region. Dictionary construction and feature extraction with discriminating texton are applied to both the center region and the periphery region. The final feature of the whole mass region is a weighted combination of the features computed from the center region and the periphery region. The proposed classification method does not need to segment the contour of each mass and directly deals with the region containing the mass. All the procedures described below are applied on the mass region, not the whole original mammogram.

The rest of this paper is organized as follows: Section 2 details the scheme of texton based classification. Section 3 proposes the discriminating texton. Section 4 gives the two-concentric masks and its application in feature extraction of the whole mass region. Section 5 presents the methodology for mass classification. In Section 6, the results and analysis are given. Section 7 summarizes the conclusions.

2. Texton

The basic idea of texton is that there are only a small number of perceptually distinguishable micro-structures at local scale in the whole image. These micro-structures can be captured by the response to a set of the filter banks [22] or by small neighborhood intensities [23]. Then an image is transformed as a histogram using these small micro-structures. A scheme of classification for texton based on neighborhood intensities is shown in Fig. 1. There are four main parts: dictionary construction, texton quantization, image representation, and classification.

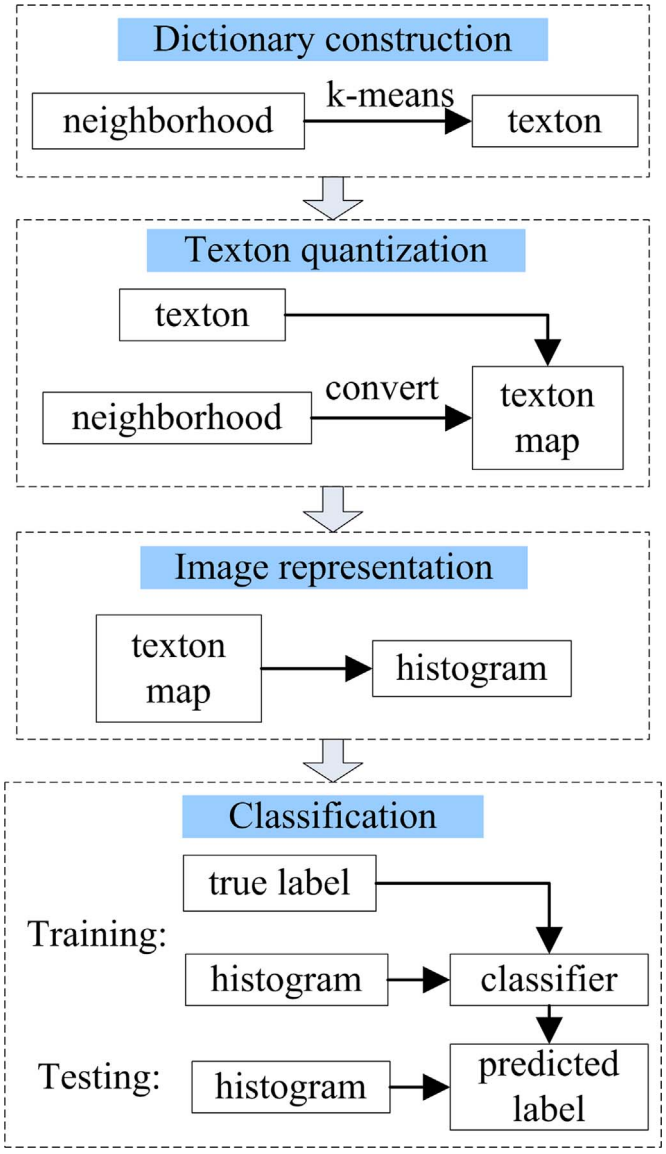

Fig. 1. The scheme of texton-based classification.

For dictionary construction, neighborhood intensities of every pixel in every training image are extracted. These neighborhoods are column vectors and aggregate together. Then the method of k-means is applied to these column vectors to find the texton dictionary. Each cluster center returned by the k-means is an element of the texton dictionary. The number of centers in the k-means is decided by the number of texton, N_{dic}. Normally the k-means is applied to each class and the final dictionary is the combination of centers for different classes. Thus the value for k in k-means equals $N_{dic}/2$. For the mass classification, all the training images are divided into benign mass class and malignant mass class. Then k-means is respectively applied to both the neighborhood vectors of the benign class and that of the malignant class.

For texton quantization, every pixel in the training and testing images is represented by its neighborhood intensities. Then these neighborhoods are quantized using the textons in the dictionary. Usually, one neighborhood is quantized to its nearest texton in the dictionary according to the Euclidean distance, given by (1).

$$L(\mathbf{G}_i) = \arg\min_j \{d(\mathbf{G}_i, \mathbf{Dic}_j)\}, \quad i = 1, \ldots, M, \quad j = 1, \ldots, N_{\text{dic}}. \tag{1}$$

In (1), $\mathbf{G}_i$ is the neighborhood intensities for pixel i. $\mathbf{Dic}_j$ is the jth element in the texton dictionary. $L(\mathbf{G}_i)$ is the texton quantization result for pixel i and lies in the range from 1 to N_{dic}. $d(\mathbf{G}_i, \mathbf{Dic}_j)$ is the Euclidean distance between $\mathbf{G}_i$ and $\mathbf{Dic}_j$. M is the number of pixels in the image.

For image representation, the texton probability distribution histogram is used to model a particular image. As images are different in size, the histogram should be normalized by the image size. For classification, a classifier such as k-nearest-neighbor (KNN) or support vector machine (SVM) is trained with the training texton histograms and their class information. The class of a testing image is then predicted using the testing texton histogram and the trained classifier.

Though texton based on neighborhood intensity has good performance, it also has its own problems. Firstly, neighborhood intensities are sensitive to the presence of illumination variation. Secondly, the class information of the training samples is not considered in the dictionary construction and the texton quantization. Thirdly, the spatial layout information is disregarded [24].

3. Discriminating texton

In texton based classification, texton dictionary is constructed by applying k-means over the neighborhoods of all the training images. As the k-means is an unsupervised learning method, the class information of all the training samples is not taken into consideration for the traditional texton. In order to add the class information of all the training samples into the texton dictionary, discriminating texton combining LDA with texton is proposed in this paper.

LDA is to find a linear combination of features which separates two or more classes of objects. The principle of LDA is to project the labeled data to a vector $\boldsymbol{w}$, which will give a maximal separation between the projected class means while also keeping the variance within each class as small as possible [25]. Using the Lagrange method, the projection vector $\boldsymbol{w}$ is solved as:

$$S_B \boldsymbol{w} = \lambda S_W \tag{2}$$

where $\boldsymbol{S}_B$ is the between-class covariance matrix and $\boldsymbol{S}_W$ is the total within-class covariance matrix.

The discriminating texton has a similar scheme with the traditional texton, except the dictionary construction and texton quantization. For the dictionary construction, a discriminating dictionary is built. First, the projection vector is computed by applying LDA to the neighborhoods of all the training samples. If the image contains a malignant mass, every neighborhood in the image is labeled as malignant. If the image contains a benign mass, every neighborhood in the image is labeled as benign. The training samples are the set of neighborhoods in all training images. After computing the projection vector $\boldsymbol{w}$, a discriminating neighborhood intensities $\mathbf{Gd}_i$ is generated and defined by (3). N is the size of the neighborhood.

$$\mathbf{Gd}_i(k) = \boldsymbol{w}(k) \bullet \mathbf{G}_i(k), \quad k = 1, \ldots, N^2. \tag{3}$$

The discriminating neighborhood is the neighborhood intensities weighted by the coefficients in LDA projection vector $\boldsymbol{w}$. Finally, the method of k-means is respectively applied to benign discriminating neighborhood intensities and malignant discriminating neighborhood intensities. The centers returned by k-means form the discriminating texton **Dic**. The flowchart of the discriminating texton generation is shown in Fig. 2.

For the texton quantization, the distance between the neighborhood intensities $\mathbf{G}_i$ and a texton in the discriminating dictionary $\mathbf{Dic}_j$ is also a little different from the traditional texton. It is the Euclidean distance between the discriminating neighborhood intensities and the texton element $\mathbf{Dic}_j$, defined by (4).

$$d(\mathbf{G}_i, \mathbf{Dic}_j) = \sqrt{\sum_{k=1}^{N^2} [\mathbf{Gd}_i(k) - \mathbf{Dic}_j(k)]^2} \tag{4}$$

4. Two-concentric masks

In texton based classification, the information about the spatial layout is disregarded. To alleviate this problem, two-concentric masks according to the mass growth characteristic are employed to divide the whole mass region into a center region and a periphery region. Then the discriminating texton is separately applied to the center region and the periphery region.

The border information is important in mass classification. When looking inside a mass, the border information exists in the outer region of a mass region. Based on this observation, two-concentric masks are designed. The masks are a set of 2-value images, bearing the same centroid and similar external boundary. Using the two-layer concentric masks, the whole mass region is divided into the center region and the periphery region. The two-concentric concentric masks are shown in Fig. 3. Fig. 3(a) is the first layer mask and corresponds to the center mask, $\mathbf{Mask}_{\text{cen}}$. The width of the center mask is half width of the mass region. The height of the mask is half height of the mass region. Fig. 3(b) is the second layer mask and corresponds to the periphery mask,

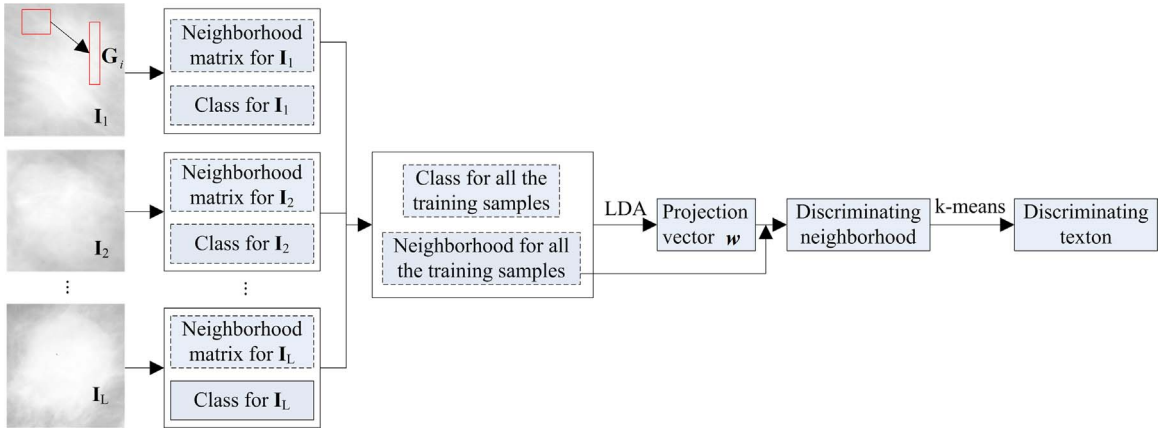

Fig. 2. The generation of discriminating texton.

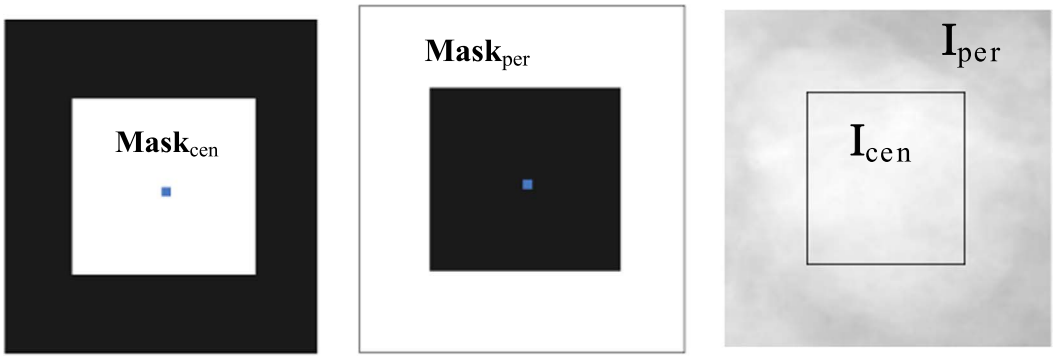

(a) the center region mask (b) the periphery region mask (c) the center region and the periphery region

Fig. 3. The two-concentric masks (a) the center region mask (b) the periphery region mask (c) the center region and the periphery region.

$\mathbf{Mask}_{\text{pre}}$. Let $\mathbf{I}$ be the gray value matrix of the mass region. The center region of $\mathbf{I}$ is computed as $\mathbf{I}_{\text{cen}}=\mathbf{I}\times\mathbf{Mask}_{\text{cen}}$ and the periphery region of $\mathbf{I}$ is computed as $\mathbf{I}_{\text{per}}=\mathbf{I}\times\mathbf{Mask}_{\text{pre}}$. Fig. 3(c) shows an example for the center region and the periphery region. Intuitively, the border information exists in the periphery region.

The center region corresponds to the interior part of a mass. The periphery region corresponds to the border part of a mass. Due to the growth characteristic of a mass, the micro-structures of the interior part and that of the border part are different. For the interior part, some homogeneous structures are normally seen. For the border part, some smooth structures are normally seen in a benign mass, shown in the rectangle of Fig. 4(a). However, some spiculate structures are normally seen in the border part in a malignant mass, shown in the rectangle of Fig. 4(b). Based on this observation, dictionary construction and feature extraction with the discriminating texton are conducted to both the center region and the periphery region.

After discriminating texton calculation, the center region and the periphery region are represented by their texton histograms, respectively. The final feature of the whole region is the combination of these two texton histograms. The periphery region corresponds to the edge part and should be more effective to tell benign mass and malignant mass apart, compared with the center region. Based on this observation, the texton histogram of the periphery region should be given more weight than the that of the center region in the feature combination. Let $\boldsymbol{h}_{\text{cen}}$ be the texton histogram of the center region and $\boldsymbol{h}_{\text{per}}$ be the texton histogram of the periphery region. The final feature of the whole mass region $\boldsymbol{f}$ is computed by (5).

$$\boldsymbol{f}=\left[\alpha\boldsymbol{h}_{\text{cen}}\ \ \boldsymbol{h}_{\text{per}}\right] \tag{5}$$

In (5), α is the regulation parameter and lies between 0 and 1.

5. Mass classification method

5.1. Classifier training

After discriminating texton calculation for the center region and the periphery region, one image was represented by a $2N_{\text{dic}}$-length feature. The first N_{dic} elements form one histogram and the second N_{dic} elements form the other histogram. In this experiment, the KNN classifier is employed for the classification step. The χ^2-distance between the feature of a training image $\boldsymbol{f}_1$ and the feature of a testing image $\boldsymbol{f}_2$ inputting to the KNN classifier is calculated by (6).

$$d(\boldsymbol{f}_1,\boldsymbol{f}_2)=0.5\bullet\sum_{j=1}^{2N_{\text{dic}}}\frac{[\boldsymbol{f}_1(j)-\boldsymbol{f}_2(j)]^2}{\boldsymbol{f}_1(j)+\boldsymbol{f}_2(j)} \tag{6}$$

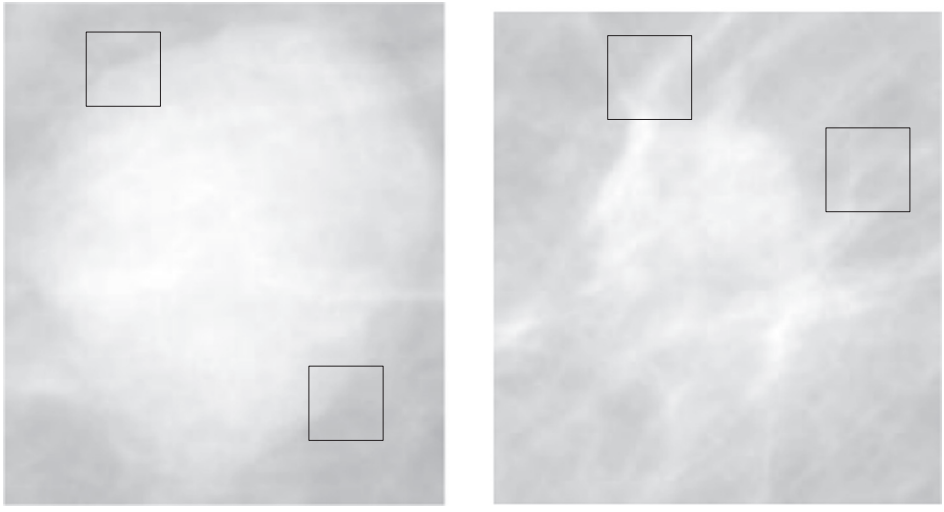

(a) the micro-structure for a benign mass (b) the micro-structure for a malignant mass

Fig. 4. The micro-structures in the border part for a benign mass and a malignant mass (a) the micro-structures for a benign mass (b) the micro-structures for a malignant mass.

5.2. The overall method

To alleviate illumination variation, the intensities of all the images are normalized in the range from 0 to 1 [26]. The proposed classification steps based on two-concentric masks and discriminating texton are as follows:

Step 1: Apply intensity normalization to all the training images and the testing images.

Step 2: Generate the two-layer concentric masks for all the training images and partition the images as the center regions and the peripheral regions.

Step 3: Extract neighborhood vectors $\mathbf{G}_{cen}$ and $\mathbf{G}_{per}$ for each pixel of the center regions and the peripheral regions in all training images, respectively.

Step 4: The construction of dictionary and the feature extraction of the training images.

Step 4.1: Apply LDA to the neighborhood vectors and their labels in the center regions ($\mathbf{G}_{cen}$) and the peripheral regions ($\mathbf{G}_{per}$) of all the training images, separately. Then the projection vector $\boldsymbol{w}_{cen}$ and $\boldsymbol{w}_{per}$ are found.

Step 4.2: Construct the discriminating dictionary for the center regions $\mathbf{Dic}_{cen}$ based on the projection vector $\boldsymbol{w}_{cen}$ and the neighborhood vector $\mathbf{G}_{cen}$.

Step 4.3: Construct the discriminating dictionary for the peripheral regions $\mathbf{Dic}_{per}$ based on the projection vector $\boldsymbol{w}_{per}$ and the neighborhood vector $\mathbf{G}_{per}$.

Step 4.4: Quantize the center regions of the training images with discriminating dictionary $\mathbf{Dic}_{cen}$ and the peripheral regions with discriminating dictionary $\mathbf{Dic}_{per}$.

Step 4.5: Represent the center region of each training image as the normalized histogram $\boldsymbol{h}_{cen}$ of the discriminating dictionary $\mathbf{Dic}_{cen}$.

Step 4.6: Represent the peripheral region of each training image as the normalized histogram $\boldsymbol{h}_{per}$ of the discriminating dictionary $\mathbf{Dic}_{per}$.

Step 4.7: Combine $\boldsymbol{h}_{cen}$ and $\boldsymbol{h}_{per}$ to generate the feature for each training image as $\boldsymbol{f}=[\alpha\boldsymbol{h}_{cen}\ \boldsymbol{h}_{per}]$.

Step 5: train a KNN classifier using $\boldsymbol{f}$ and the class information with all the training images.

Step 6: Using Step 2–3, extract neighborhood vector for each pixel of the center region and the peripheral region in one testing image, respectively.

Step 7: Using Step 4.4–4.7, generate the feature for the testing image as $\boldsymbol{f}_t$.

Step 8: Input the feature of the testing image $\boldsymbol{f}_t$ to the trained KNN classifier and predict its label.

An overview of the proposed methodology is given in Fig. 5.

6. Results and analysis

6.1. Image dataset

Mammograms downloaded from the DDSM database [27] were used to test the proposed method. A subset of DDSM masses scanned on LUMISYS digitizer was selected from the malignant cancer volumes and the benign volumes. The resolution of these mammograms was 50 μm/pixel at 12 bits/pixel. To reduce the processing time, all the images were down sampled to a resolution of 100 μm/pixel. For classification, a mass region image was cropped from the original mammogram as the minimum rectangle containing a mass. The mass regions provided by DDSM are usually larger than the true region. Thus, the region images used in this paper were cropped by a radiologist under the contours provided by DDSM. The experiment has been implemented on a Lenovo workstation with a 2.4 GHz processor of two cores.

Since the DDSM cases were acquired at different clinical sites, cases were selected from different volumes to balance the potential population difference. These compose a total of 130 mass regions, of which 52 are benign masses and 78 are malignant masses. The density distribution of the masses is shown in Fig. 6. Some examples of the mass regions are shown in Fig. 7.

6.2. Parameter setting

A "5-fold" cross validation scheme was employed to test the classification performance. It randomly divided the whole dataset into 5 groups. Four groups were used for the training images and one group for the testing images. This process was repeated 5 times (the folds), and each of the 5 groups was used exactly once as the testing images. Parameters and their values used in this experiment are shown in Table 1. The optimized value of the parameter set was the one bearing the maximum training classification accuracy. For the number of textons in the dictionary, smaller N_{dic} creates fewer textons. This dictionary may not be enough to represent the whole dataset. Larger N_{dic} creates more textons. This dictionary may include redundant textons. To balance the trade-off, the value range for N_{dic} was set from 60 to 100. For the neighborhood size N, there is no a good criterion for choosing a fixed value. According to [23], N equal of 3, 5, and 7 was tested.

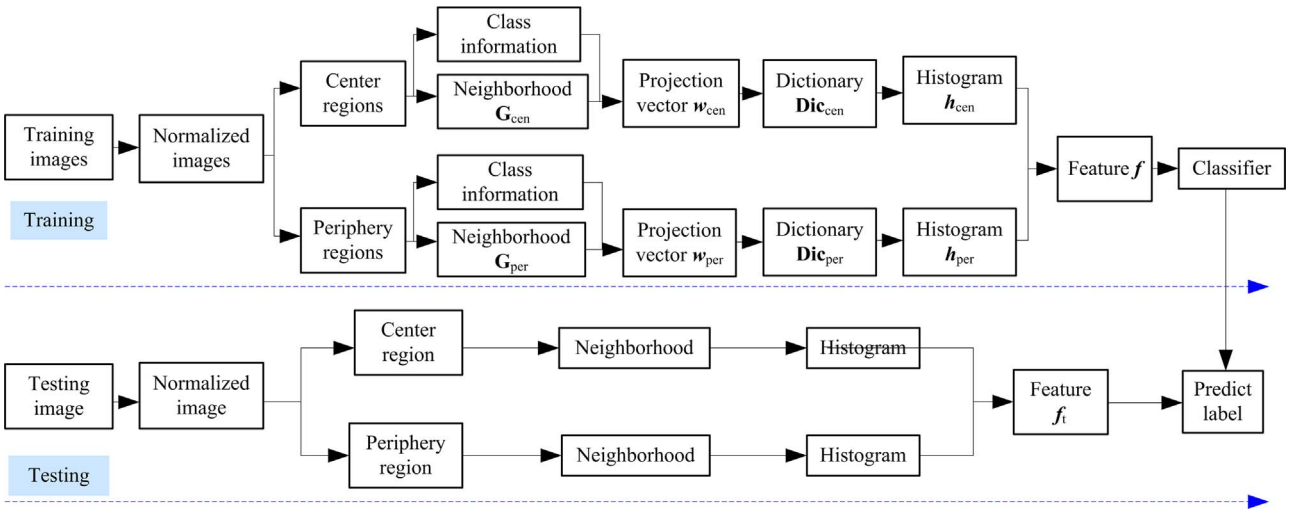

Fig. 5. The whole method for mass classification.

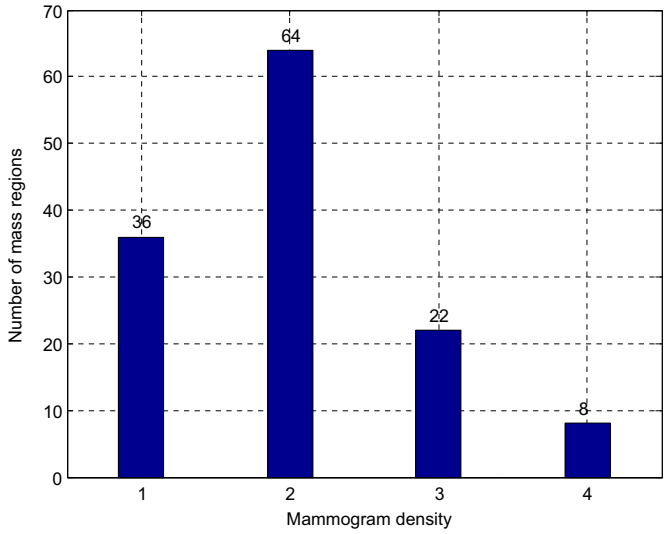

Fig. 6. Density distribution of masses. Mammogram densities 1–4 are quantitative assessment of breast density according to BI-RADS. They represent almost entirely fatty breast, scattered areas of fibroglandular, heterogeneously dense breast and extremely dense breasts.

For the regulation parameter α, when α is 0, the influence of the center region disappears. When α equals to 1, the influence of the center region and the periphery region becomes the same. To better combine the histogram of the center region and that of the periphery region, a reasonable range for α may be from 0.6 to 0.9. For the KNN classifier, the parameter k was set as 3, experimentally.

6.3. Evaluation criteria

Three criteria are used to evaluate the proposed classification method. The first criterion is the classification accuracy rate. The second criterion is sensitivity (*Sens*) and specificity (*Spec*). The definitions of TP, FN, TN and FP are given in [18].

$$Sens = \frac{TP}{TP + FN}, \quad Spec = \frac{TN}{TN + FP}. \tag{7}$$

The third criterion is the area under the Receiver operating characteristics (ROC) curve A_z. ROC curve is generated as the plots of true positive rate (TPR) vs. false positive rate (FPR). Using different thresholds, a set of TPR and FPR pairs are derived.

Table 1
Parameters.

K-means (N_{dic})	Neighborhood size (N)	α	KNN(k)
60–100	3–7	0.6–0.9	3

6.4. Analysis of the proposed method

The first comparison is to test the importance of adding spatial layout information and discriminating information. Traditional texton and the proposed method were conducted on the same dataset. The accuracy, sensitivity, specificity and the area under the ROC curve for these two methods are shown in Table 2. It can be seen that the accuracy and the specificity are improved by using the proposed method. The sensitivity for these two methods are almost the same. The results may be explained as follows. The interior part of a mass may display some spiculate structures, formed by the superposition of some glandular tissues. Traditional texton equally treats the spiculate structures in the interior part and that in the edge part. Thus some benign masses are classified as malignant ones. Classifying a benign mass as a malignant one is more acceptable than classifying a malignant mass as a benign one. Thus a smaller center region may be better. A quarter or other

(a) Malignant mass regions

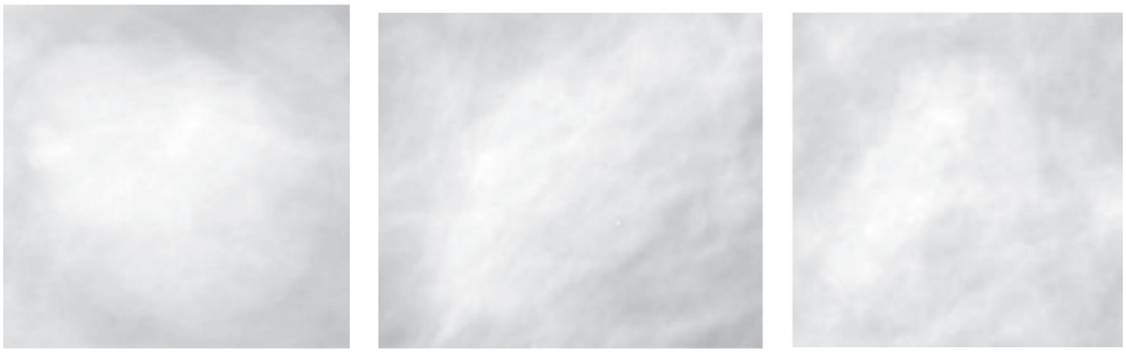

(b) Benign mass regions

Fig. 7. Regions containing a malignant mass (a) or a benign mass (b). (a) Malignant mass regions (b) Benign mass regions.

Table 2
Comparisons of different texton-based methods.

	Acc (%)	*Sens* (%)	*Spec* (%)	A_z
Traditional texton	80.77	88.46	69.23	0.85
Cen-texton	63.08	79.49	38.46	0.73
Per-texton	77.69	83.33	69.23	0.83
Spatial texton	83.08	87.18	76.92	0.88
Proposed method	86.92	87.18	86.54	0.91

size of the whole mass region will be discussed in the future.

The second comparison is to test which part of the whole mass is more effective to tell benign mass and malignant mass apart. Classification were conducted on the same dataset, using features extracted from the center region, the periphery region and the combination of these two regions. For a simplified description, mass classification using features extracted from the center region are called cen-texton and that from the periphery region are called per-texton. The accuracy, sensitivity, specificity and the area under the ROC curve are shown in Table 2. From Table 2, the periphery region is more effective to tell the benign mass and the malignant mass apart than the center region. The reason may be that the border information is included in the periphery region. Another observation was that the combination of these two regions was more effective than the periphery region itself. From this observation, we may conclude that the center regions between a benign and a malignant mass were also different. Texton features extracted from the center region also have the discriminating ability.

The third comparison is to test the importance of constructing dictionary individually for the center region and the periphery region. First, a new dictionary was generated by clustering the neighborhoods of the whole region. Then features were individually extracted for the center region and the periphery region using the new dictionary. For a simplified description, feature generated by this method is called spatial texton. Spatial texton and the proposed method were conducted to classify benign masses and malignant masses. The accuracy, sensitivity, specificity and the area under the ROC curve are shown in Table 2. The accuracy and the specificity of spatial texton are lower than the proposed method. The sensitivity for these two methods are the same. The results may be explained as follows. The texton dictionaries constructed by the whole region is similar to that constructed by the periphery region. Thus the classification performance of the malignant masses are the same for the two methods. The second observation is that the texton dictionaries of the center region is different from the that of the periphery region. Thus the classification performance of the benign masses for the proposed method is higher than spatial texton.

6.5. Comparisons between our method and existing methods

To further evaluate the ability of the proposed method, several existing methods for mass classification are also tested for comparison. As the proposed method is done without segmenting the contour of each mass, just texture-based methods are employed in this comparison. The selected methods are GLCM [10], SRD [11], wavelet [12], Gabor [16], LPQ [17] and majority voting texton (MV-texton) [18] based method. Different methods are tested on different databases. For comparisons, we repeat these methods on our database and compare their performance using the *Acc* and A_z. All these methods were trained and tested using KNN classifier and a "5-fold" cross validation scheme. For wavelet, we tested several wavelet functions and the one giving the highest accuracy rate was chosen. For LPQ, several variants were tested. The highest accuracy rate was obtained using three-scale LPQ. For MV-texton, the results reported in [18] were used. The first reason is that the database used in [18] and that used in this paper are overlapped a lot. Second, the computation time for the whole procedure in [18] is too large. The comparison results are shown in Table 3. The ROC curves for these methods are drawn in Fig. 8.

Table 3
Comparison with existing methods.

	Acc (%)	A_z
GLCM [10]	63.08	0.63
SRD [11]	66.92	0.69
Wavelet [12]	63.85	0.65
Gabor [16]	71.54	0.74
LPQ [17]	67.69	0.69
MV-texton [18]	85.96	0.92
Proposed method	86.92	0.91

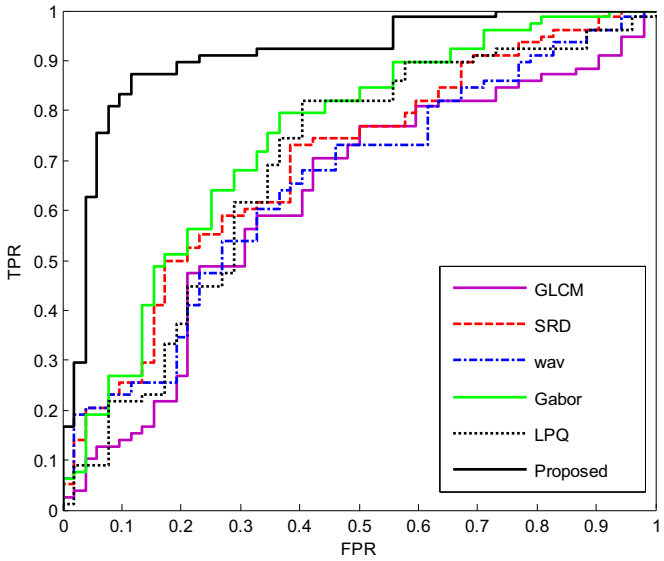

Fig. 8. ROC curves for different methods.

Table 3 shows that the classification performance of the proposed method is higher than that of the existing methods when the mass contours are not segmented. This revealed the effectiveness of the proposed method. The reason may be that the extracted features for the existing methods were computed from the whole mass region. However, for a benign or a malignant mass, the characteristics of its interior part and outer part are different.

.Our previous work [18] and the proposed method are different adaptions on original texton. The method in [18] deals with the scale dependent problem in original texton. This problem is alleviated by majority voting on different non-uniform subsamplings. The proposed method deals with two problems. The first problem is the unsupervised learning of the dictionary construction in original texton. It is alleviated by adding the discriminating information learned by LDA. This solution may be also effective in other classification problems using texton feature extraction. The second problem is the disregard of spatial layout information. It is alleviated by designing the two-concentric masks based on the growth characteristics of a mass. This solution may be effective for mammographic mass classification using other features. Besides, the efficiency of [18] is lower than the proposed method. The non-uniform subsamplings and majority voting by different subsamplings contribute to the low efficiency. For the proposed method, the average time of feature extraction for one image is 7 s. For the method in [18], the average time of feature extraction for one image is 28 s. Thus in the proposed method, non-uniform subsamplings and majority voting are not used.

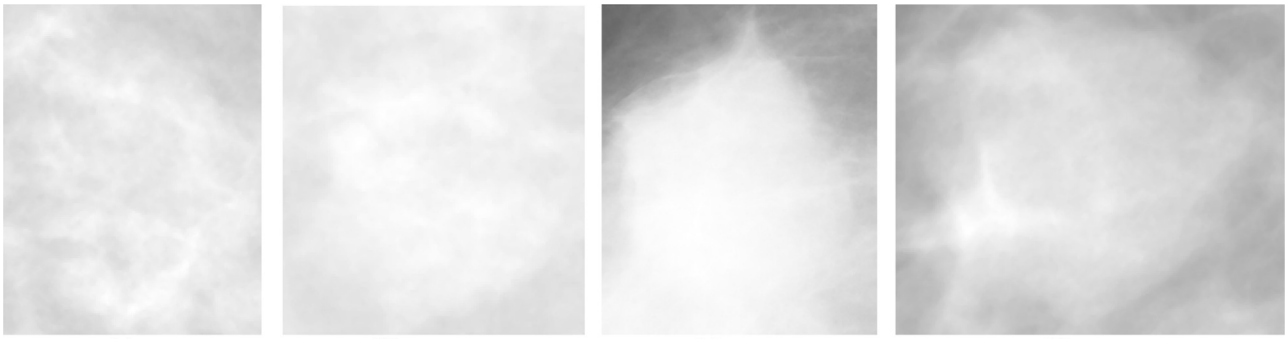

Fig. 9. Masses that are not correctly classified.

6.6. Analysis of incorrect classification

Though the result of the proposed method seems satisfactory for the most part, some problems also exist. Some examples of masses that are not correctly classified are shown in Fig. 9. Firstly, some masses are overlapped by the glandular tissues. The mass border is not obvious. For this type of masses, the proposed method cannot get correct classification, as shown in Fig. 9(a) and (b). The reason may be that the micro-structures for these masses are similar. Secondly, some malignant masses may have round or oval shape shown in Fig. 9(c) and some benign masses may have some spiculate structure shown in Fig. 9(d). For these masses, the proposed method may also get incorrect classification results. The reason may be that the micro-structures for spiculate benign masses are commonly seen in a malignant mass. The micro-structures for oval malignant masses are commonly seen in a benign mass.

7. Conclusions

In this paper, an effective mass classification method is proposed by combining two-concentric masks with discriminating texton. This method does not need to segment the contour of each mass and has two advantages. First, the dictionary construction and texton quantization are unsupervised learning process in traditional texton scheme. To solve this problem, the discriminating texton is proposed integrating LDA with traditional texton. Second, the spatial layout information is disregarded in traditional texton scheme. To solve this problem, two-concentric masks according with the mass growth characteristic are employed to divide the whole mass region as the center region and the periphery region. Dictionary construction and feature extraction are applied to both the center region and the periphery region with discriminating texton. When experimented on 130 mass regions, the proposed method shows an improvement in mass classification compared with traditional texton and some existing methods. Two other observations can also be concluded. First, the periphery region is more effective to tell benign mass and malignant mass apart than the center region. Second, respectively applying texton to the periphery region and the center region is more suitable than applying texton to the whole mass region when classifying mass as benign or malignant.

Acknowledgment

This work was supported in part by the National Natural Science Foundation of China 61271305, 61502025, the China Postdoctoral Science Foundation 2015M570029 and the Fundamental Research Funds for the Central Universities of China 2015RC024.

References

[1] B. Verma, P. McLeod, A. Klevansky, A novel soft cluster neural network for the classification of suspicious areas in digital mammograms, Pattern Recognit. 42 (2009) 1845–1852.
[2] X. Zhou, H. Huang, S.L. Lou, Authenticity and integrity of digital mammography images, Med. Imaging IEEE Trans. 20 (2001) 784–791.
[3] R.M. Rangayyan, T.M. Nguyen, Fractal analysis of contours of breast masses in mammograms, J. Digit. Imaging 20 (2007) 223–237.
[4] R.M. Rangayyan, N.R. Mudigonda, J.L. Desautels, Boundary modelling and shape analysis methods for classification of mammographic masses, Med. Biol. Eng. Comput. 38 (2000) 487–496.
[5] R.M. Rangayyan, N.M. El-Faramawy, J.L. Desautels, O. Alim, Measures of acutance and shape for classification of breast tumors, Med. Imaging IEEE Trans. 16 (1997) 799–810.
[6] T. Mu, A.K. Nandi, R.M. Rangayyan, Classification of breast masses using selected shape, edge-sharpness, and texture features with linear and kernel-based classifiers, J. Digit. Imaging 21 (2008) 153–169.
[7] D. Guliato, R.M. Rangayyan, J.D. Carvalho, S. Santiago, Polygonal modeling of contours of breast tumors with the preservation of spicules, Biomed. Eng. IEEE Trans. 55 (2008) 14–20.
[8] A.K. Mohanty, M.R. Senapati, S.K. Lenka, A novel image mining technique for classification of mammograms using hybrid feature selection, Neural Comput. Appl. 22 (2013) 1151–1161.
[9] A.K. Mohanty, M.R. Senapati, S. Beberta, S.K. Lenka, Texture-based features for classification of mammograms using decision tree, Neural Comput. Appl. 23 (2013) 1011–1017.
[10] J.A. Jaleel, S. Salim, S. Archana, Textural features based computer aided diagnostic system for mammogram mass classification, in: Control, Instrumentation, Communication and Computational Technologies (ICCICCT), 2014 International Conference on, 2014, pp. 806–811.
[11] S. Shanthi, V.M. Bhaskaran, A novel approach for detecting and classifying breast cancer in mammogram images, Int. J. Intell. Inf. Technol. 9 (2013) 21–39.
[12] M.Z. do Nascimento, A.S. Martins, L.A. Neves, R.P. Ramos, E.L. Flores, G. A. Carrijo, Classification of masses in mammographic image using wavelet domain features and polynomial classifier, Expert Syst. Appl. 40 (2013) 6213–6221.
[13] M.M. Eltoukhy, I. Faye, B.B. Samir, A comparison of wavelet and curvelet for breast cancer diagnosis in digital mammogram, Comput. Biol. Med. 40 (2010) 384–391.
[14] M.M. Eltoukhy, I. Faye, An optimized feature selection method for breast cancer diagnosis in digital mammogram using multiresolution representation, Appl. Math. 8 (2014) 2921–2928.
[15] M. Hussain, S. Khan, G. Muhammad, G. Bebis, A comparison of different gabor features for mass classification in mammography, in: Signal Image Technology and Internet Based Systems (SITIS), 2012 Eighth International Conference on, 2012, pp. 142–148.
[16] M. Hussain, G.M. Salabat Khan, I. Ahmad, G. Bebis, Effective extraction of gabor features for false positive reduction and mass classification in mammography, Appl. Math. Inf. Sci. 6 (2012) 29–33.
[17] L. Nanni, S. Brahnam, A. Lumini, A very high performing system to discriminate tissues in mammograms as benign and malignant, Expert Syst. Appl. 39 (2012) 1968–1971.
[18] Y. Li, H. Chen, G.K. Rohde, C. Yao, L. Cheng, Texton analysis for mass classification in mammograms, Pattern Recognit. Lett. 52 (2015) 87–93.
[19] A.M. Abdel-Zaher, A.M. Eldeib, Breast cancer classification using deep belief networks, Expert Syst. Appl. 46 (2016) 139–144.
[20] A. Ahmadvand, M.R. Daliri, Rotation invariant texture classification using

extended wavelet channel combining and LL channel filter bank, Knowl.-Based Syst. 97 (2016) 75–88.
[21] A. Ahmadvand, M.R. Daliri, Invariant texture classification using a spatial filter bank in multi-resolution analysis, Image Vis. Comput. 45 (2016) 1–10.
[22] T. Leung, J. Malik, Representing and recognizing the visual appearance of materials using three-dimensional textons, Int. J. Comput. Vis. 43 (2001) 29–44.
[23] M. Varma, A. Zisserman, Texture classification: Are filter banks necessary? Computer vision and pattern recognition, 2003 IEEE computer society conference on, vol. 692, 2003, II-691-698.
[24] S. Battiato, G.M. Farinella, G. Gallo, D. Ravì, Spatial Hierarchy of Textons Distributions for Scene Classification. Advances in Multimedia Modeling, Springer 2009, pp. 333–343.
[25] C.M. Bishop, Pattern Recognition and Machine Learning, Springer Science, New York 2006, pp. 179–196.
[26] C. Chen, J.A. Ozolek, W. Wang, G.K. Rohde, A general system for automatic biomedical image segmentation using intensity neighborhoods, J. Biomed. Imaging 8 (2011) 1–12.
[27] ⟨http://marathon.csee.usf.edu/Mammography/Database.html⟩.

Yanfeng Li received the B.S. and the Ph.D. degrees from Beijing Jiaotong University, China. Her research interests focus on pattern recognition and biomedical image processing.

Houjin Chen received the B.S. degree from Lanzhou Jiaotong University, China, and the M.S. and Ph.D. degrees from Beijing Jiaotong University, China. His current research interests include signal processing, machine learning and neural networks.

Xueye Wei received the B.S. and the M.S. degrees from Tianjin University, China, and the Ph.D. degree from Beijing Institute of Technology, China. His current research interests include signal processing, measurement and control.

Yahui Peng received the B.S. and the M.S. degrees from Tsinghua University, China, and the Ph.D. degree from University of Chicago, USA. His research interests focus on machine learning, pattern recognition, and biomedical applications.

Lin Cheng received the B.S. degree from Zhengzhou University, China, and the Ph.D. degree from Peking University, China. His current research interests include the diagnosis and treatment of the breast cancer.